nature climate change

LETTERS

PUBLISHED ONLINE: 28 SEPTEMBER 2014 | DOI: 10.1038/NCLIMATE2381

Detection and impacts of leakage from sub-seafloor deep geological carbon dioxide storage

Jerry Blackford, Henrik Stahl, Jonathan M. Bull *et al.*†

Fossil fuel power generation and other industrial emissions of carbon dioxide are a threat to global climate[1], yet many economies will remain reliant on these technologies for several decades[2]. Carbon dioxide capture and storage (CCS) in deep geological formations provides an effective option to remove these emissions from the climate system[3]. In many regions storage reservoirs are located offshore[4,5], over a kilometre or more below societally important shelf seas[6]. Therefore, concerns about the possibility of leakage[7,8] and potential environmental impacts, along with economics, have contributed to delaying development of operational CCS. Here we investigate the detectability and environmental impact of leakage from a controlled sub-seabed release of CO_2. We show that the biological impact and footprint of this small leak analogue (<1 tonne CO_2 d^{-1}) is confined to a few tens of metres. Migration of CO_2 through the shallow seabed is influenced by near-surface sediment structure, and by dissolution and re-precipitation of calcium carbonate naturally present in sediments. Results reported here advance the understanding of environmental sensitivity to leakage and identify appropriate monitoring strategies for full-scale carbon storage operations.

Geological CO_2 storage is proposed in deep, porous, sedimentary formations, 1–2 km below the sea floor, such as depleted oil and gas reservoirs or saline aquifers[3,4]. Storage integrity is provided by impermeable layers of cap-rock[3]. Although debated, a number of mechanisms potentially facilitating leakage have been proposed, including abandoned exploratory boreholes, geological discontinuities (for example, fractures) and operational malfunction (blowout scenario)[9]. Here we do not address storage integrity, but focus on the likely environmental consequence of leakage, and how best to detect leakage if it were to reach the marine environment.

Research on excess CO_2 in marine systems is frequently based on laboratory experiments and studies of natural CO_2 seeps[10,11]. However, laboratory studies omit physical, ecological and behavioural complexity, which are key in understanding and regulating impacts. Further, volcanic CO_2 seeps are compromised by impurities and atypical thermal, topographical and sedimentological properties[12], and the initial evolution of CO_2 flow is not known. Early detection of leakage that has reached the seabed from deep CCS storage formations is crucial for assurance, and monitoring must be viable in complex hydrodynamic environments. Consequently, we conducted a shallow controlled sub-seabed CO_2 release to replicate small-scale, but realistic, leakage that has migrated into the near-seabed environment. A borehole was drilled from shore, to a depth of 11 m beneath the sea floor, in 12 m of water and 350 m offshore (Supplementary Fig. 1). A total of 4.2 tonnes of CO_2 was injected into the overlying unconsolidated sediments, over a 37 day period, during which flow was increased from 10 to 210 kg d^{-1}. The temporal and spatial migration and impact of this CO_2 release were assessed using a variety of acoustic, chemical and biological techniques, before, during and after release at both control and exposed sites (see Methods and Supplementary Table 1). The experimental results are directly applicable to most global offshore storage sites[3], which are planned for shelf seas with water depths up to 200 m. CO_2 phase chemistry and benthic biogeochemical processes are consistent across this depth interval.

The physical movement of the injected CO_2 through the seabed was clearly imaged (Fig. 1). Within hours of commencing CO_2 injection, small gas bubble plumes were observed at the sea floor. Seismic imaging of the sediments revealed a layered structure consisting of 8 m of fine laminated mud, overlain by 2 m of fine silty sand with 1–2 m of coarse-grained sand and gravel forming the seabed (Fig. 1a, inset). Repeated seismic reflection surveys showed that during the first 13 days of release, with CO_2 injection between 10 and 80 kg d^{-1}, most CO_2 was confined to a vertical gas 'chimney' in the lower laminated mud (Fig. 1a). Within these muds, fracture propagation, or reactivation of pre-existing fractures is inevitable and rapid once a critical pressure is exceeded. This is dependent on sediment cohesiveness, injection rate and cumulative gas flux[13–15]. Thus, chimneys are interpreted to represent a laterally restricted (that is, 5–10 m wide) network of interconnected fractures (Fig. 1c). The change in grain size from mud to overlying silt and sand caused a step-change from a fracture-dominated flow regime to one dominated by capillary invasion[15] and fluidization with lower permeability. This is evidenced by the observed accumulation and lateral spread of gas at the top of the laminated mud layer (Fig. 1c, green outline). The absence of reflectance signals in the upper layers during early stages of the release is consistent with slow diffusion of gas. The initial flow of CO_2 into the water column is restricted and thought to occur through pre-existent micro fractures, beyond the resolution of seismic imaging. The increased injection rate (210 kg d^{-1}) applied during the second half of the experiment permits gas to fracture the silty sand layer (Fig. 1b), and permeate through the seabed's coarse-grained sand and gravels, consistent with chimneys extending from the injection point to the sea floor. Consequently sub-surface flow becomes more spatially focused with time as the flow rate increases (Fig. 1c, pink outline).

Rapid dissolution of gaseous CO_2 into sea water significantly increases bottom-water CO_2 partial pressure close to the injection site, with values varying between 380 and 1,500 μatm, depending on the state of the tide and injection rate, compared with background values of 360–370 μatm (Fig. 2b). The flux of gaseous CO_2 across

† A full list of authors and affiliations appears at the end of the paper.

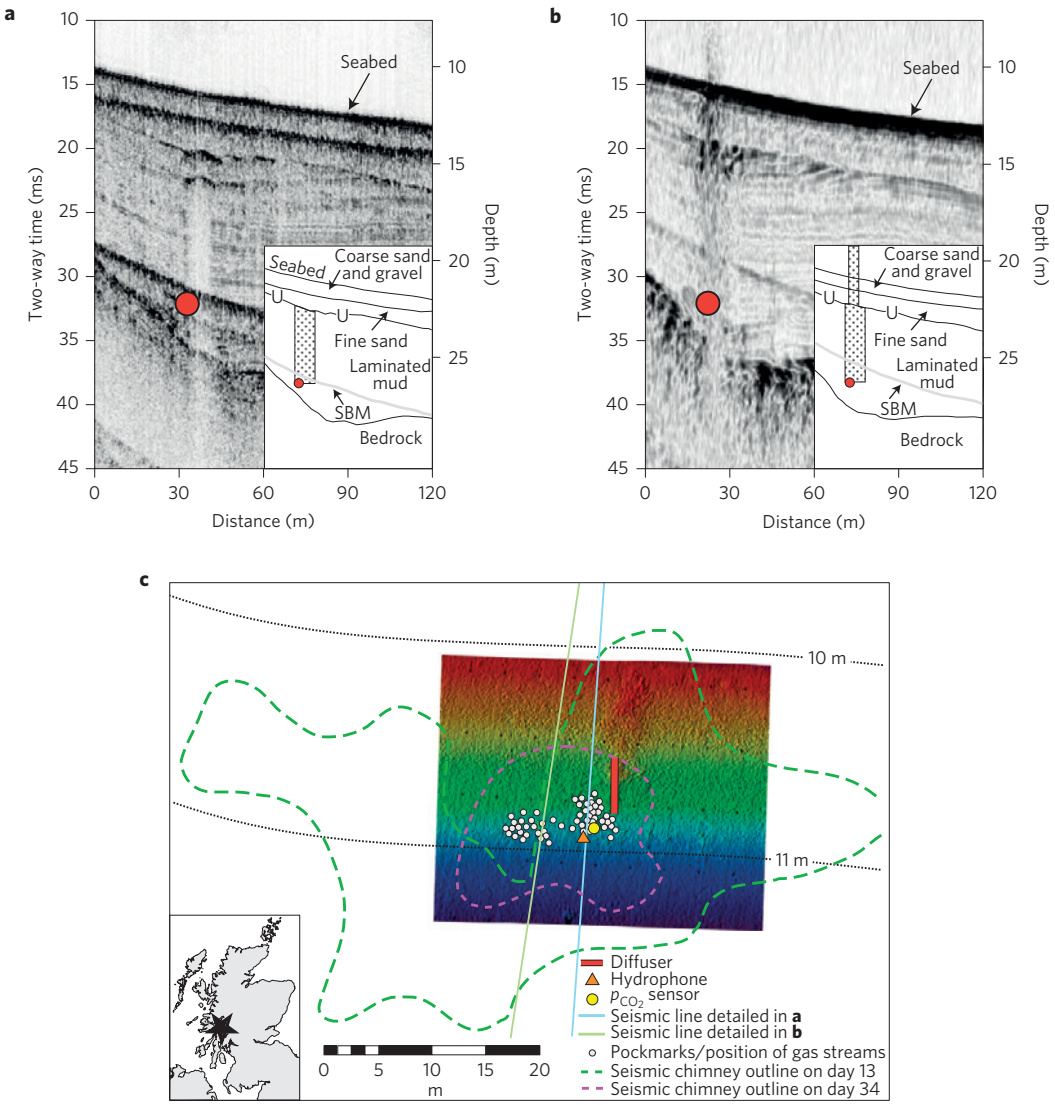

Figure 1 | Seismic reflection profiles and seabed mapping illustrating gas pathways above the CO_2 diffuser. The position of the diffuser 11 m beneath the seabed is indicated by the red dots and red line. Insets show line drawing interpretations. The seabed multiple (SBM) is an artefact. **a**, Day 13. The data image a bright spot beneath the fine sand layer. This is interpreted as free gas being trapped beneath the unconformity (U), and no gas is imaged in the water column. **b**, Day 34. Enhanced reflectivity above the diffuser, and acoustic turbidity from the diffuser to the seabed and into the water column are interpreted as free gas. **c**, Plan-view multibeam image of CO_2 leakage at the seabed on day 34. Gas-emitting pockmarks sit within the area of the chimneys imaged by seismic reflection data on day 13 and day 34. The sub-surface flow became more spatially focused with time as the flow rates were increased. The locations of the hydrophone and p_{CO_2} instruments (data shown in Fig. 2) are indicated. (Supplementary Fig. 1).

the sea floor was determined directly by divers collecting bubbles from each bubble stream, and estimated by acoustic inversion of hydrophone data[16]. On day 33, direct measurements yielded an estimated total CO_2 flow of 31.8 kg d^{-1} (Fig. 2c). At this time the input into the system was 210 kg d^{-1}; hence, only ~15% of total CO_2 was being emitted in a gaseous phase across the sediment–water interface. Gaseous CO_2 flow rates estimated from acoustic inversion (Fig. 2c) varied significantly with tidally induced changes in hydrostatic pressure (Fig. 2a), agreeing well with observations from time-lapse photography and p_{CO_2} data (Fig. 2b), and with flow determined by diver measurement. The 24 h rolling-average acoustically inferred gas flux responds consistently to the increased injection rate on day 31 (Fig. 2c) and suggests that outgassing of 15% of the total injected CO_2 was representative of the entire release phase.

The chemical response in the sediment pore waters was complex. CO_2-induced chemical changes in the biotic upper 25 cm of pore waters were not observed until the last week of the CO_2 injection period, and persisted for a maximum of two weeks after the release was stopped. During this period, dissolved inorganic carbon (DIC, dissolved CO_2 and associated inorganic carbon species) increased by a factor of ten from typical values of 2.6 mmol kg^{-1} to 29.3 mmol kg^{-1} approximately 20 cm below the sediment surface (Fig. 3a). Coincident increased concentrations of pore-water alkalinity and calcium ions (Ca^{2+}; Fig. 3b,c) indicate that the injected CO_2 that dissolves promotes rapid dissolution of calcium carbonate ($CaCO_3$), naturally present in the sediments. In corroboration of this, pore-water acidity (pH) initially drops slightly from 7.7 to 7.5, and then increases to 7.8 just after the injection was stopped (Fig. 3e), indicating that the rise in DIC was buffered by the carbonate dissolution. Carbon isotopic composition of pore-water DIC at the release epicentre ($\delta^{13}C_{DIC} = \sim -20‰$) was significantly lower than background pore water ($\sim -2‰$), which confirms that changes

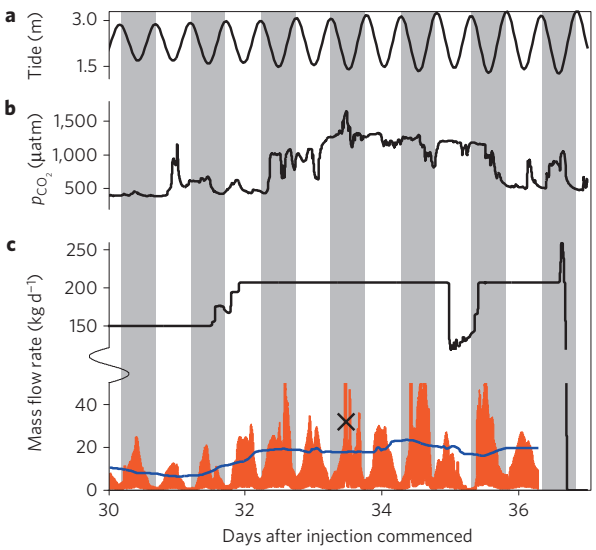

Figure 2 | Gas injection rate, hydrophone-determined seabed flux, and carbonate system variations in the water column over multiple tidal cycles during the later stages of injection. p_{CO_2} and seabed gas flux correlates with the tidal cycle, with low gas flux at high tide. **a**, Height of tidal cycle in metres. **b**, Variation in p_{CO_2} 5 cm above the seabed. **c**, Total gas injection flux (kg d^{-1}, solid black line); estimate of gas flux at the seabed from inversion of hydrophone data (orange area 25th and 75th percentiles of confidence interval; 24 h rolling mean—solid blue line). See Supplementary Methods for details on the inversion. Direct diver measurement of gas flux on day 33 (between 11:00 and 11:49) is shown by the black cross. Data are illustrated for the period between day 30 and day 36 of the release.

in pore-water carbonate chemistry were caused by the injected CO_2 ($\delta^{13}C = -26.6‰$, Fig. 3d). All pore-water carbonate chemistry parameters, including $\delta^{13}C_{DIC}$, returned to background values within 17 days of ceasing the CO_2 injection, probably owing to a combination of re-precipitation[17] of $CaCO_3$, physical and biological pore-water advection[18,19] or sinking of slightly dense CO_2-rich pore water[20].

Although changes in concentrations of pore-water DIC and Ca^{2+} in response to CO_2 were observed from 2 to 25 cm depth in the sediments, concentrations remained near background values in the top 2 cm of sediment throughout the experiment (Fig. 3a,c) and benthic chamber measurements of DIC fluxes across the sea floor showed no change from normal values[21] (Supplementary Fig. 2). Hence, we conclude that the portion of injected CO_2 that does not escape from the sediments in the gas phase (that is, ~85%) was retained within the sediments for the duration of the experiment. Although some of this was observable as free gas using acoustic imaging (Fig. 1), the high solubility of CO_2 would suggest that much of the injected gas was rapidly dissolved in sediment pore waters.

As high CO_2 is known to impact many biological processes[22], we investigated the degree to which chemical changes from leakage might impact biological systems, in and around the seabed. Seabed communities naturally change, sometimes significantly, throughout the seasonal cycle (Fig. 4, black lines). Impact is indicated not by change per se, but by deviations from well-established normal cycles. No biological effect was detected during the initial stages of the release, consistent with the lack of a chemical signal in the superficial sediments. However, towards the end of the release and in the initial days of the recovery period, the change in benthic macrofauna community structure at the leak epicentre (Fig. 4, red lines) was significantly different from that observed at the

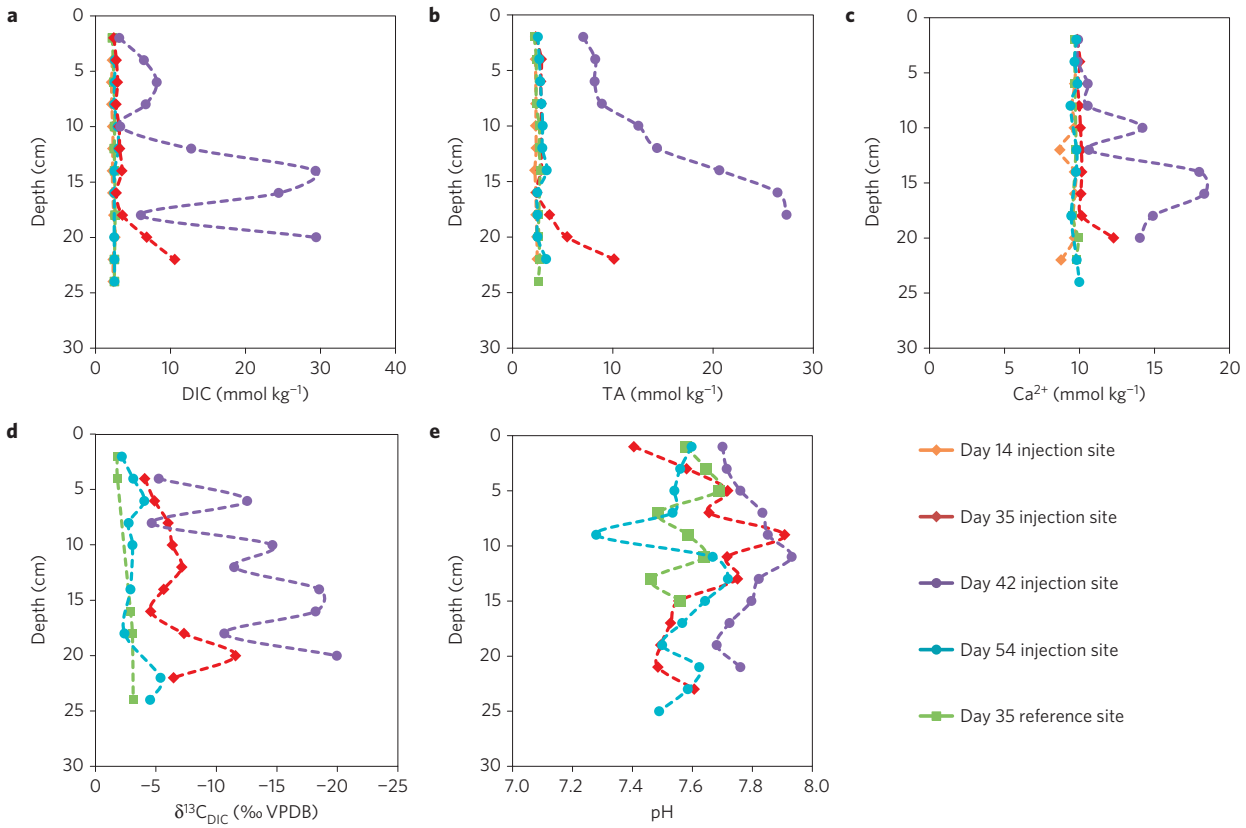

Figure 3 | Temporal evolution of dissolved carbonate system parameters in sediment pore water at the injection site (zone 1). Data are shown for day 14 and day 35 during the injection phase and at 5 days and 17 days after the gas release ceased (day 42 and day 54 of the experiment respectively). A typical profile from the control site (zone 4, day 35, green line) is also shown for comparison. **a**, DIC. **b**, Total alkalinity (TA). **c**, Ca^{2+}. **d**, Carbon isotopic composition of DIC ($\delta^{13}C_{DIC}$). **e**, pH. Deviations from control values (green) are apparent only on days 35 and 42.

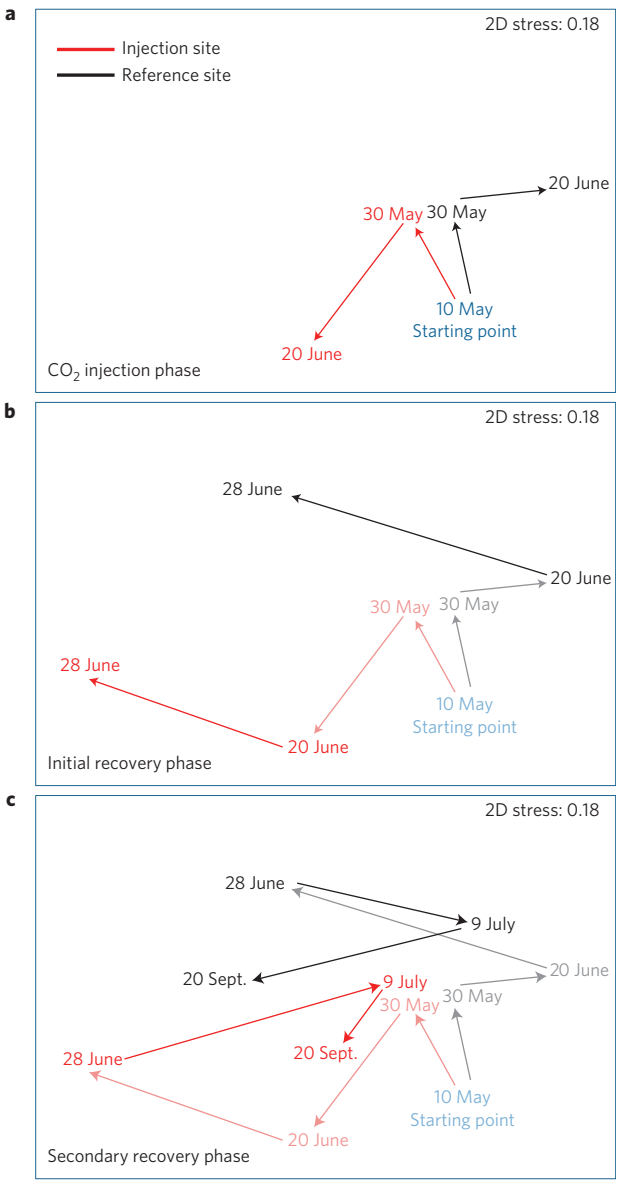

Figure 4 | A multi-dimensional (MDS) plot comparing temporal changes in benthic macrofaunal community structure at the release site with the reference sites. In an MDS plot, similar biological communities in terms of biodiversity and abundance (represented by dates) appear close together and parallel trajectories (arrows) represent comparable changes. Dissimilarity is represented by greater spatial separation or diverse trajectories. **a**, During the initial stages of leakage, until 30 May community development is similar at both impacted and reference sites; however, in the later stages of the injection, significant divergence is apparent. **b**, During the initial stages of recovery, until 28 June both impacted and non-impacted communities show similar trajectories, but remain dissimilar in make-up. **c**, In the later stages of recovery convergence between all communities is apparent. The generation of MDS plots is detailed further in the Methods; the reference data represent an average of the three separate non-impacted sites.

other, un-impacted sites. Intermittently the high-CO_2 plume in the water column was advected 25 m from the epicentre owing to tidal circulation, inducing transitory changes in carbonate chemistry. Here bacterial gene expression in the top 1 cm of sediment responded similarly to that at the leakage epicentre (Supplementary Fig. 3), indicating a rapid sensitivity of the active bacterial community. No other CO_2 impact was recorded away from the release epicentre at any stage. The dominant biological variability at both release and control sites was the normal seasonal dynamic; at the end of the sampling period no significant difference between impacted and non-impacted communities was apparent in the macrofauna (Fig. 4c), although differences in the gene expression of microbial populations persisted for at least 90 days (Supplementary Fig. 3).

Our work demonstrates that biological effects from a small short-term leak are detectable, but not catastrophic and that recovery is measurable in days to weeks. The restricted vertical and horizontal effect of our small-scale leak is not without parallel. The effects of natural seepage of methane into the water column from cold seeps such as pockmarks and mud volcanoes on continental margins are restricted to a narrow zone that extends only a few metres from the seep epicentre[23,24]. The distribution of bacterial communities and macrofauna at these seeps is principally controlled by the rate of fluid flow[25,26], and the bacterial communities respond rapidly to changes in environmental conditions[27].

We caution that impacts are likely to increase step-wise if a greater proportion of CO_2 is emitted in the gaseous phase, either through fractures or as pore waters become super-saturated, or if the carbonate buffering capacity of the sediments is limited or becomes exhausted. Without operational evidence, realistic leakage scenarios can only be approximated. Based on natural gas seepage and offshore drilling, estimates range from ~20 tonnes per annum (half the experimental release rate) for seepage through abandoned wells to short-term leakage of 50 kilotonnes d^{-1} for highly unlikely blowout scenarios[9]. Modelling-derived estimates of the footprint of biologically harmful plumes of CO_2 indicate that high end scenarios may impact a few kilometres radius[28] whereas lower end scenarios, consistent with this experiment, will impact only some metres in radius[29]. For all leakage scenarios so far examined, models indicate that hydrodynamic mixing would disperse harmful concentrations of CO_2 within hours to weeks, facilitating recovery as excess CO_2 is not accumulated in biological tissues unlike most toxic substances. Siting storage below restricted exchange environments, where dispersion is limited, could lead to significant build-up of CO_2-charged water[12] and should be avoided.

Monitoring the large volume of sea water overlying a geological storage complex will be challenging. We show that low levels of leakage dominated by dissolution and subsequent transport of CO_2 by diffusion may be hard to detect and quantify, owing to carbonate buffering. Small seabed pockmarks are an early indication of leakage, but these features can be difficult to distinguish from natural biogenic structures. Bubble streams, when present, are easily recorded, but we observed that these are sensitive to hydrostatic pressure and may represent a fraction of released CO_2. Although seismic and chemical signals over an established leakage locus will be distinct, given the restricted horizontal and vertical footprint of leakage, spatial coverage and the ability to measure signals near the seabed will be paramount for monitoring. Furthermore, natural biologically and physically driven variability of CO_2 in marine systems[30] and sediment heterogeneity may render detection of signals at small distances from leakage loci hard to discriminate, unless a rigorous baseline is established.

We suggest that the optimal monitoring strategy for storage locations should use mobile autonomous underwater vehicles equipped with chemical (for dissolved phase) and acoustic (for gas bubbles) sensors with a horizontal spatial sampling resolution approaching 10 m, deployed close to the sea floor. Such a multi-sensor approach, supported by analysis against a well-constrained baseline will maximize the chance of detecting the preliminary stages of a small leakage. Should specific higher risk, spatially restricted, leakage sites be identified, a network of permanently deployed long-term stable online sensors and hydrophones may provide the most effective monitoring tools for early leak detection.

Once a suspected leak is detected, alternative techniques should be implemented to corroborate the source (for example, by sensors and isotopic signature); to quantify fluxes of CO_2 (for example, by acoustic inversion for gas and sediment-pore-water incubations for dissolved phase); and to assess associated impacts (for example, by biological sampling). Baseline studies therefore need to encompass sediment structure and carbonate content, natural seeps, the acoustic background, CO_2 chemistry and biological community structure within the context of seasonal and spatial heterogeneity.

We do not address the robustness of deep geological storage in this work, but provide an insight into the processes that occur if leaked CO_2 were to reach the shallow unconsolidated sediments immediately underlying the seabed. This emerging understanding synthesizing dispersion, impact and recovery suggests that small-scale leakage from CCS, should it reach the sea floor, is highly unlikely to have a regionally significant environmental impact. Although monitoring may be challenging, it is tractable given a multivariate approach, supported by appropriate baseline studies.

Methods

The experiment site, located on the west coast of Scotland (Supplementary Fig. 1, inset), fulfilled multiple criteria including access and logistics, regulatory release permissions, local approval, suitable seabed geology and sediments with diverse fauna typical of regional shelf seas. Extensive high-resolution seismic reflection profiling and sediment core sampling were instrumental in site selection and subsequently fully characterized the site for drilling operations. A 350-m-long borehole, subsequently lined with stainless-steel pipe was drilled through quartzite bedrock using a directional drilling rig, avoiding glacial till deposits and natural accumulations of biogenic gas, with the final 10 m terminating horizontally into unconsolidated sediments (Supplementary Fig. 1). The borehole terminated in a 5-m-long diffuser with multiple perforations of 0.5 mm diameter, to ensure diffuse flow of gas into the surrounding sediments. The diffuser was positioned 11 m below the seabed and beneath a further 10–12 m of water, dependent on tide height. The land-based facilities comprised CO_2 cylinders; connected by manifolds, regulated by a high-precision mass-flow controller, logging at 12 s periodicity. Initial injection was commenced at 10 kg CO_2 d^{-1} to avoid hydraulic fracturing, increasing to 210 kg CO_2 d^{-1} to achieve a realistic flux and biogeochemically significant signal at the seabed. The total injection amounted to 4.2 tonnes over a 37 day period.

Surveying used a combination of boat-towed instrumentation, diver-mediated sampling and semi-permanently deployed instrumentation on the sea floor. Sampling was undertaken at four bathymetrically and ecologically similar zones (zone 1: epicentre, zone 2: 25 m distant, zone 3: 75 m distant, zone 4: 450 m distant acting as a control, Supplementary Fig. 1). The sites were investigated immediately before the start of CO_2 release; during the 37 day release period; and over one year after termination of the release (Supplementary Table 1).

High-resolution seismic reflection data comprised 194 Boomer and Chirp profiles, covering an area of 600 by 400 m centred above the diffuser location, with a 5–10 m line separation. A calibrated hydrophone was deployed close to the diffuser to record the acoustic signature of gas bubbles emitted from the seabed within the water column.

CO_2 fluxes across the sediment–water interface were quantified by direct diver collection, a passive acoustic inversion technique[16] based on hydrophone data and benthic chambers for quantifying DIC flux. The partial pressure of CO_2 in the water column was monitored by a calibrated p_{CO_2} ion-sensitive field-effect transistor electrode[31] moored at 5 cm height above the seabed at the centre of the release site.

Sediment samples for pore-water biogeochemistry analysis, including DIC, total alkalinity, pH, isotopic composition ($\delta^{13}C_{DIC}$), Ca^{2+} and biological samples, were manually collected in shallow cores by divers. At each zone and time point five replicate cores were analysed for microbial and macrofaunal populations. Fauna were analysed to the lowest taxonomic level possible. Microbial RNA was extracted and analysed using terminal restriction fragment length polymorphism; a molecular biology technique commonly used to profile microbial communities, based on the position of a restriction site closest to a labelled end of the 16S ribosomal RNA gene.

This study uses a non-parametric multivariate approach, MDS, which characterizes and compares faunal samples on the basis of the identity and abundance of macrofaunal species (Fig. 4) or microbial 16S rRNA gene T-RF (terminal restriction fragment) relative abundances (Supplementary Fig. 3). Ordinations are derived from Bray–Curtis similarity matrices using an MDS technique[32,33]. The Bray–Curtis measure ignores joint absences and focuses on presences and is the most commonly used similarity matrix for biological community analyses. An MDS ordination is essentially a map of samples in which the distance between any two samples is a reflection of their relative similarity to each other based on the whole community composition. Thus, samples positioned closely to each other are very similar in community composition, and points that are further apart are less similar in their composition. The goodness of fit of the ordination (given that a multi-dimensional distribution is compressed to a two-dimensional one) is indicated by a stress value. Values below 0.2 imply that the ordinations may be sensibly interpreted. As this technique is based on the rank order in the similarity matrix, it is only the relative distance apart of the symbols that matters, the scale and axis being arbitrary.

An animation of the experimental procedure and video footage of seafloor bubble streams and instrumentation can be seen at www.qics.co.uk. Supplementary Table 1 summarizes the sampling regime and further details are given in the Supplementary Information.

Received 10 June 2014; accepted 22 August 2014; published online 28 September 2014

References

1. IPCC *Third Assessment Report of the Intergovernmental Panel on Climate Change (IPCC)* (Cambridge Univ. Press, 2001).
2. Raupach, M. R. *et al.* Global and regional drivers of accelerating CO_2 emissions. *Proc. Natl Acad. Sci. USA* **104,** 10288–10293 (2007).
3. IPCC in *IPCC Special Report on Carbon Dioxide Capture and Storage* (eds Metz, B., Davidson, O., de Coninck, H. C., Loos, M. & Meyer, L. A.) 442 (Cambridge Univ. Press, 2005).
4. Senior, B. CO_2 Storage in the UK—Industry Potential, DECC, URN 10D/512, 2010.
5. Nakanishi, S. *et al.* Methodology of CO_2 aquifer storage capacity assessment in Japan and overview of the project. *Energy Procedia* **1,** 2639–2646 (2009).
6. Austen, M. C. *et al. The UK National Ecosystem Assessment Technical Report* (UNEP-WCMC, 2011).
7. Van Noorden, R. Carbon sequestration: Buried trouble. *Nature* **463,** 871–873 (2010).
8. Monastersky, R. Seabed scars raise questions over carbon-storage plan. *Nature* **504,** 339–340 (2013).
9. IEA Greenhouse Gas R&D Programme (IEA GHG) Assessment of sub-sea ecosystem impacts (2008).
10. Widdicombe, S., Blackford, J. C. & Spicer, J. I. Assessing the environmental consequences of CO_2 leakage from geological CCS: Generating evidence to support environmental risk assessment. *Mar. Pollut. Bull.* **73,** 399–401 (2013).
11. Caramanna, G., Voltattorni, N. & Maroto-Valer, M. Is Panarea Island (Italy) a valid and cost-effective natural laboratory for the development of detection and monitoring techniques for submarine CO_2 seepage? *Greenhouse Gases: Sci. Technol.* **1,** 200–210 (2011).
12. Carey, S. *et al.* CO_2 degassing from hydrothermal vents at Kolumbo submarine volcano, Greece, and the accumulation of acidic crater water. *Geology* **41,** 1035–1038 (2013).
13. Boudreau, B. P. *et al.* Bubble growth and rise in soft sediments. *Geology* **33,** 517–520 (2005).
14. Algar, C. K., Boudreau, B. P. & Barry, M. A. Initial rise of bubbles in cohesive sediments by a process of viscoelastic fracture. *J. Geophys. Res.* **116,** B04207 (2011).
15. Jain, A. K. & Juanes, R. Preferential mode of gas invasion in sediments: Grain-scale mechanistic model of coupled multiphase fluid flow and sediment mechanics. *J. Geophys. Res.* **114,** B08101 (2009).
16. Leighton, T. G. & White, P. R. Quantification of undersea gas leaks from carbon capture and storage facilities, from pipelines and from methane seeps, by their acoustic emissions. *Proc. R. Soc. A* **468,** 485–510 (2012).
17. Mucci, A. *et al.* Fate of carbon in continental shelf sediments of eastern Canada: A case study. *Deep-Sea Res. II* **47,** 733–760 (2000).
18. Aller, R. C. & Aller, J. Y. The effect of biogenic irrigation intensity and solute exchange on diagenetic reaction rates in marine sediments. *J. Mar. Res.* **56,** 905–936 (1998).
19. Janssen, F., Huettel, M. & Witte, U. Pore-water advection and solute fluxes in permeable marine sediments (II): Benthic respiration at three sandy sites with different permeabilities (German Bight, North Sea). *Limnol. Oceanogr.* **50,** 779–792 (2005).
20. Duan, Z., Hu, J., Li, D. & Mao, S. Densities of the CO_2–H_2O and CO_2–H_2O–NaCl systems up to 647 K and 100 MPa. *Energ. Fuel.* **22,** 1666–1674 (2008).
21. Anderson, L. G. *et al.* Benthic respiration measured by total carbonate production. *Limnol. Oceanogr.* **31,** 319–329 (1986).
22. Gattuso, J. P. & Hansson, L. (eds) *Ocean Acidification* 326 (Oxford Univ. Press, 2011).

23. DeBeer, D. *et al. In situ* fluxes and zonation of microbial activity in surface sediments of the Håkon Mosby mud volcano. *Limnol. Oceanogr.* **51,** 1315–1331 (2006).
24. Lichtschlag, A. *et al.* Methane and sulfide fluxes in permanent anoxia: *In situ* studies at the Dvurechenskii mud volcano (Sorokin Trough, Black Sea). *Geochim. Cosmochim. Acta.* **74,** 5002–5018 (2010).
25. Decker, C. *et al.* Habitat heterogeneity influences cold-seep macrofaunal communities within and among seeps along the Norwegian margin. Part 1: Macrofaunal community structure. *Mar. Ecol.* **33,** 205–230 (2012).
26. Gruenke, S. *et al.* Niche differentiation among mat-forming, sulfide-oxidizing bacteria at cold seeps of the Nile Deep Sea Fan (Eastern Mediterranean Sea). *Geobiology* **9,** 330–348 (2011).
27. Felden, J. *et al.* Limitations of microbial hydrocarbon degradation at the Amon mud volcano (Nile deep-sea fan). *Biogeosciences* **10,** 3269–3283 (2013).
28. Blackford, J. C., Jones, N., Proctor, R. & Holt, J. Regional scale impacts of distinct CO_2 additions in the North Sea. *Mar. Pollut. Bull.* **56,** 1461–1468 (2008).
29. Dewar, M., Wei, W., McNeil, D. & Chen, B. Small scale modelling of the physiochemical impacts of CO_2 leaked from sub-seabed reservoirs or pipelines within the North Sea and surrounding waters. *Mar. Prod. Bull.* **73,** 504–515 (2013).
30. Thomas, H. *et al.* Controls of the surface water partial pressure of CO_2 in the North Sea. *Biogeosciences* **2,** 323–334 (2005).
31. Shitashima, K., Kyo, M., Koike, Y. & Henmi, H. *Proceedings of the 2002 International Symposium on Underwater Technology* 106–108 (IEEE, 2002).
32. Clarke, K. R. Non-parametric multivariate analyses of changes in community structure. *Aust. J. Ecol.* **18,** 117–143 (1993).
33. Kruskal, J. B. & Wish, M. *Multidimensional Scaling* (Sage Publications, 1978).

Acknowledgements

Funding was provided by NERC (NE/H013962/1), the Scottish Government and METI/MEXT of Japan. We thank the Tralee Bay Holiday Park, Lochnell Estates and the inhabitants of Benderloch for hosting the experiment. We acknowledge Marine Scotland and The Crown Estate for permissions to carry out the research. The NERC National Facility for Scientific Diving, the crew of the RV *Seol Mara* and J. Montgomery based at SAMS provided operational support. We thank A. Skinner of ACS coring services for advice on the drilling, and the design of the well screen; J. Davis for support of geophysical data acquisition; C. Wallace of Kongsberg Ltd for provision and processing of the multibeam bathymetry data; J. Gafiera (BGS) for interpretation of site survey seismic profiles and A. Monaghan (BGS) for construction of 3D geological models.

Author contributions

R.H.J., D.C., H.S., S.W., K.S., A.L., P.T., J.K., C.H., K.T., M.S. and M.H. designed and undertook biogeochemical measurements and analysed data; M.C., M.E.V., I.W., D.L., D.S., J.M.B. and M.A. planned, acquired and interpreted seismic reflection data; T.G.L., P.R.W. and B.J.P.B. designed and undertook passive acoustic measurements, analysed data and completed gas flux inversion; T.M.G. analysed and interpreted core data; B.C. analysed bubble dynamics from bottom photographs; M.D.J.S. led the diving deployment and sampling strategy; B.C., H.K. and T.S. developed models to constrain the experimental deployment; D.L., D.S. and M.A. developed the concept, design and implementation of the borehole and gas delivery mechanism; H.S., P.T. and M.N. designed and built the CO_2 injection facility; H.S. led and coordinated the release and sampling strategy; J.B., H.S., I.W., R.H.J., J. K., B.C., C.H., S.W. and M.N. conceived the study; J.B. led the project; D.S., B.J.P.B., M.C. and A.L. produced figures within the manuscript; J.B., H.S. and J.M.B. developed and co-wrote the manuscript. All authors discussed results and commented on the manuscript.

Additional information

Supplementary information is available in the online version of the paper. Reprints and permissions information is available online at www.nature.com/reprints. Correspondence and requests for materials should be addressed to J.B.

Competing financial interests

The authors declare no competing financial interests.

Jerry Blackford[1]*‡, Henrik Stahl[2]‡, Jonathan M. Bull[3]‡, Benoît J. P. Bergès[4], Melis Cevatoglu[3], Anna Lichtschlag[5], Douglas Connelly[5], Rachael H. James[3], Jun Kita[6], Dave Long[7], Mark Naylor[8], Kiminori Shitashima[9], Dave Smith[7], Peter Taylor[2], Ian Wright[5], Maxine Akhurst[7], Baixin Chen[10], Tom M. Gernon[3], Chris Hauton[3], Masatoshi Hayashi[11], Hideshi Kaieda[12], Timothy G. Leighton[4], Toru Sato[13], Martin D. J. Sayer[2,14], Masahiro Suzumura[15], Karen Tait[1], Mark E. Vardy[3], Paul R. White[4] and Steve Widdicombe[1]

[1]Plymouth Marine Laboratory, Prospect Place, Plymouth PL1 3DH, UK, [2]Scottish Association for Marine Science, Oban PA37 1QA, UK, [3]Ocean and Earth Science, University of Southampton, National Oceanography Centre Southampton, Southampton SO14 3ZH, UK, [4]Institute of Sound and Vibration Research, Engineering and the Environment, University of Southampton, Highfield, Southampton SO17 1BJ, UK, [5]National Oceanography Centre, University of Southampton Waterfront Campus, Southampton SO14 3ZH, UK, [6]Research Institute of Innovative Technology for the Earth, 9-2, Kizugawadai, Kizugawa-Shi, Kyoto 619-0292, Japan, [7]British Geological Survey, Murchison House, West Mains Road, Edinburgh EH9 3LA, UK, [8]School of GeoSciences, Grant Institute, University of Edinburgh, Edinburgh EH9 3JW, UK, [9]International Institute for Carbon-Neutral Energy Research, Kyushu University, 744 Motooka, Nishi-ku, Fukuoka 819-0395, Japan, [10]School of Engineering & Physical Sciences, Heriot-Watt University, Edinburgh EH14 4AS, UK, [11]The General Environmental Technos Co., Ltd., 1-3-5 Azuchimachi, Chuo-ku, Osaka 541-0052, Japan, [12]CRIEPI, 1646 Abiko, Abiko-shi, Chiba 270-1194, Japan, [13]Department of Ocean Technology, Policy and Environment, University of Tokyo, 5-1-5, Kashiwanoha, Kashiwa-shi, Chiba 277-8561, Japan, [14]NERC National Facility for Scientific Diving, Scottish Association for Marine Science, Oban PA37 1QA, UK, [15]National Institute of Advanced Industrial Science and Technology, 16-1 Onogawa, Tsukuba, Ibaraki 305-8569, Japan. ‡These authors contributed equally to this work. *e-mail: jcb@pml.ac.uk